ACTIVITY OF COMET HALE–BOPP (1995 01) 13 EYOND6 AU FROM THE SUN

Z. Sekanina

Jet Propulsion Laboratory, California Institute of Technology
Pasadena, CA 91109, U.S.A.

December 1995

Submitted to
Astronomy & Astrophysics
(Main Journal)

Abstract

The physical evolution of comet Hale–Bopp is investigated along the preperihelic arc of its orbit at heliocentric distances larger than 6 AU. The comet's considerable intrinsic brightness and activity are explained by the existence of a relatively large area on its nucleus surface that is a reservoir of both carbon monoxide and dust particulates. Three recurring dust emission events observed in August–October 1995 are studied in some detail. The characteristic shape of the features generated in the course of these episodes is interpreted as a product of a sharply peaked diurnal emission profile and suggests a probable common source to all the three events. The timing of the events' sequence is shown to exhibit a periodicity that may be diagnostic of the comet's state of rotation, which apparently is not pure spin. The total mass of dust ejected during one of the episodes is calculated from reports of the comet's "(nuclear magnitudes" at pertinent times to be on the order of 10^{11} grams. Estimates of the dust production rate are compared with the published production rates of carbon monoxide and it is concluded that the mass loading of the CO gas flow by dust was enormous, certainly much greater than 15. Finally, comet Hale–Bopp is compared with other comets known to have experienced activity at large heliocentric distances. Most similarities are found with the dust emission pattern of comet 29 P/Schwassmann-Wachmann 1.

1. introduction

Not often have visual observers an opportunity to monitor a 10th-rnagnitude cometary object at a heliocentric distance of 7 AU. Comet Hale-Bopp offered such a chance in the second half of]995, thanks apparently to the existence of a sizable area on its nucleus surface with abundant supplies of both carbon monoxide and dust-- the prime subject of this study. Other issues addressed include: (i) the temporal evolution of dust emission events, three of which were extensively observed between late August and late October 1995; (ii) the amount of dust ejecta's mass involved in the events and computer modelling of observed dust features; (iii) the nature of the emission mechanism and a working model for the comet's outgassing pattern; and (iv) comparison with some other comets that arc known to '(suffer" from a propensity for outbursts at large distances from the Sun.

2. Observed phenomena

Following its discovery on July 23, 1995, the comet was unusually bright and exhibited an asymmetric coma (Offutt 1995), which prompted Sekanina (1995a) to suggest that shortly before the first observations the comet had undergone a major outburst, similar in nature to those known to be experienced from time to time by 29P/Schwassmann-Wachmann 1, and that both the elevated brightness and the halo were products of the emission episode.

Because of the interference from the Moon, relatively few observations were made during the first half of August. A major development (hereafter referred to as Event 1) was reported independently and almost simultaneously by Jewitt and Chen (1995), by Fitzsimmons and Cartwright (]995), by Kidger et al. (1995) (cf. also Kidger 1995a), and by West (1995): numerous high-resolution images taken between August 24 and at least September 8 showed consistently a radial, rectilinear jet emerging from the nucleus condensation to the west-northwest, turning sharply to the north at a distance of several seconds of arc from the center, and terminating in a gradually fading spiral arm that vanished in the first quadrant. The radial jet's position angle was reported to be between 280° and 315° (on the average, 2900-295") and the spiral arm's maximum extent to the north was measured to be ~10 arcsec.

Evidence for a new burst of significant activity (Event 2) was detected on images taken between September 26 and October 2 (Kidger 1995a,b, McNaught 1995). The feature's outlines are seen most clearly on images taken by Weaver (1995) with the Hubble Space Telescope's (11ST) Wide Field Planetary Camera 2 (WFPC-2) on September 26.67 UT. The "tip" of the rectilinear jet appears on a composite image as a somewhat elongated concentration of mass ~1 arcsec across, centered on a point 1.4 arcsec from the nucleus at a position angle of ~325°. 'l'he feature's evolution followed closely the pattern observed during Event 1, except that the radial jet now was at a position angle of 320°-3250, some 25°-350 to the north relative to its orientation in late August/early September. The claim of the jet's rapid rotation (Kidger 1995a) was soon retracted (Kidger 1995 b).

Finally, signs of apparently the last preconjunction outburst (Event 3) were noticed first on images taken on October 14-]5 (Kidger 1995b) and the feature's extremely faint traces were barely detected still on another set of HST images taken on October 23.27 U"J', after the intensity scale was "stretched" to an extreme (Weaver 1995). The feature's development was once again virtually the same as before, the jet pointing this time almost exactly to the north. An extensive depository of this comet's images from J uly-October 1995 is located at URI, http://newproducts.jpl.nasa.gov/comet/images.html.

3. Model scenarios for the evolution of the emission events

As pointed out in the early short reports (Sekanina 1995b), the type of spiral features observed is characteristic of temporally limited ejection of dust from discrete sources on the sunlit side of a rotating nucleus. The proposed model for the three emission events is based primarily on several fundamental findings. First of all, solar radiation pressure effects on microscopic dust, particles are insignificant at the large heliocentric distances and on the time scales of several days involved. Hence, the curvature of the spiral arm is due to rotational variations in the ejection velocity vector field during each emission episode and the particles could not be emitted from a polar region of the nucleus, while the equatorial zone is acceptable. The feature's oval-shaped boundary is a rnca.sure of the angle that the comet's apparent spin vector subtended with the Earth's direction during the event and the orientation of the feature contour's boundary determines the projected spin vector's approximate position angle. The azimuthal extent of the spiral arm, about 90°, indicates that the emission of dust continued for about one quarter of the apparent rotation period, but the effective spin rate itself remained for all practical purposes indeterminate, with only crude constraints possible, as discussed in Sect. 4.

Since the bright radial jet was projected generally toward the Sun, it is reasonable to assume that it represented the direction of emission from the discrete source near the time of its transit across the subsolar meridian. If the source was located near the equatorial plane, the 90° azimuthal extent of the observed spiral allows two emission scenarios: either the source was activated near local sunrise and deactivated near local noon, or it was activated around noon and decativatcd around sunset. Qualitatively, physical considerations favor the latter scenario, even though a gross topographic obstruction (e.g., a precipitous cliff), suddenly setting off or shutting off the sunlight's access to the source, can about equally well explain the late (midday) "ignition" or the early (midday) termination of the event, should the dust emission rate depend very critically on the Sun's local elevation. The advantage of the preferred emission profile is its logical interpretation of the production peak's short duration, followed by a gradual decrease in the ejecta's injection rate and by the episode's eventual termination near sunset, This scenario may indicate the rejuvenation, during the diurnal window of dormancy, of a limited reservoir of volatile ices and dust in the source region, with most of the supplies expended soon after the event had been allowed by the local topography to begin– hence a brief, sharp production peak. In the other scenario- with the episode assumed to have lasted from sunrise to midday- -the dust production would first be increasing only gradually, then peaking sharply just before the event's sudden termination (due again, presumably, to a topographic barrier). The physical reasons for the appearance of a sharp peak *at the end* of a period of slow production growth arc not intuitively obvious, And since a *sudden* production drop is hardly an expected signature of the process of a reservoir's *gradual* depletion, one expects that, in the course of the next emission event, the production rate would reach its peak shortly after activation- contrary to observational evidence.

The feature's slow expansion implies low dust-particle velocities, not exceeding some 30 m/s in projection onto the plane of the sky. The relative prominence of the outer boundary of the feature suggests a fairly steep particle size distribution of the dust, with a significant excess of the smallest (micron-sized or smaller) grains that left the nucleus with the highest expansion velocities. The surface brightness of the ejects during the sharp production peak was sufficient for this general region of the emission feature to be detected in its entirety, including the near-nucleus areas that were populated by larger particles whose projected expansion velocities were substantially lower than 3(I m/s.

With the subsequent sudden drop in the production rate the surface brightness decreased correspondingly and only the most prominent part of the halo--its outer boundary- remained visible. The feature's characteristic shape is thus a product of the *event's* distinctive diurnal emission profile.

One observed property of the dust feature that the proposed emission scenario cannot as yet explain, is the systematic rotational motiorr of the radial jet from a position angle of ~290° during Event 1 to ~320° during Event 2 and to ~0° during Event 3. To account for this effect and a parallel rotation of the spiral arm, an additional constrain! needs to be introduced. Perhaps the most obvious choice at first sight is the possibility that the three emission episodes had their origin in three different active regions on the nucleus surface, as proposed by Kidger (1995 c). However, two lines of evidence point against this interpretation. One is the remarkably similar appearance of the features resulting from the three events, the other is the relative timing of the episodes, which shows a very distinct pattern (Sect. 4). For these reasons, I attribute all three episodes to a single discrete source. If so, the rotational motions of the radial jet and the spiral arm then require that the nucleus be in a complex state of rotation, the rate of precession of one body axis about the angular momentum vector and the rate of (complete or incomplete) roll of that axis being nearly- but not perfectly- -commensurable. This state of rotation leads to systematic variations in the observed geometry of the ejected material that superficially mimick the source's migration over the nucleus surface on the assumption of pure spin.

4. Computer simulation of the evolution of the dust ejecta

The synthetic images of the evolving spiral features, generated by applying the developed computer simulation technique (e.g., Sekanina 1991, 1996 and references therein) and presented for selected observation times in Fig. 1, arc based on the information that was summarized in Sect. 3. The primary source of data for Event 1 was the computer processed version of the image taken by E.Molinari with the Danish 154-cm telescope at the European Southern Observatory on August 31.06 UT (West 1995). This image was complemented by information from cursory inspection of numerous additional images from the period August 24 through September 6. The basic data on Event 2 were provided by the HST image from September 26 and by Kidger's (1995b) length measurements of the radial jet, while the principal source of information on Event 3 was the HST image from October 23.

One of the objectives of this study is to offer synthetic images that show a reasonable degree of similarity with the evolution of the dust features observed following the three major emission events. It is not the objective of these modelling efforts to *optimize* the solutions in every respect, although they arc the result of much experimentation especially with respect to temporal variations in the apparent dimensions of the features.

To facilitate the computer image simulations in the absence of more comprehensive information, the presented model is based on two major restrictions that make the results valid only approximately: (i) the complex state of rotation a precession and a roll- are assumed ***during the emission episode*** to be crudely equivalent to pure spin along an axis whose inertial position varied from event to event and is to be determined by the best fit between model and observation; and (ii) the apparent spin rate ***during the emission episode is*** constant. The degree of correspondence between model and observation is nearly insensitive to the spin rate and the only parameters that are affected are the beginning and end times of the emission events.

The fundamental commonalities for all three emission episodes are: (i) a single source, located at a fixed apparent latitude of the nucleus; (ii) emission occurring during the same time of the day, from local noon to local sunset; (iii) a universal diurnal emission profile; (iv) essentially a fixed range and a fixed distribution law of dust-particle accelerations due to solar radiation pressure, β; (v) a universal functional law between the accelerations β and the ejection velocities of the dust particles, v_{eject}; and (vi) an invariable apparent spin rate. The assumption of each episode's activation from noon to sunset, combined with the assumptions of the source's fixed apparent latitude and a constant spin rate, implies that the three emission events were of equal durations. The only fundamental parameters allowed to vary from episode to episode were, of course, the absolute times of the event's onset and termination and, as mentioned, the position of the apparent spin vector.

The common and individual parameters arc for the three events listed in 'Table 1, 'The upper limit to the particle acceleration β, which has no practical effect on the quality of fit, is at best only marginally constrained by existing color observations of the comet's dust and it was chosen to allow for micron-, possibly submicron-sized grains. Hicks (1995) measured essentially solar values for the .7--11 and $J-K$ magnitudes on July 27 in fields 12 to 24 arcsec in diameter centered on the nucleus. Lidman and Bouchet (1995) found the comet to be colorless, that is, significantly bluer than the Sun, in the same near-infrared spectral region and in a somewhat smaller aperture on August 5. Temporally the most relevant observations for investigations of Event 1, made by Fomenkova and Mumma (1995) on September 1, indicate that the signal from the near-nuclear region less than 3000 km in radius had a color index $J-K \approx 0.2$ mag, thereby being only slightly bluer than the Sun.

'l'he variable step in the solar radiation pressure acceleration β was chosen to mimick a differential distribution law varying as an inverse $5\frac{1}{2}$th power of particle size, which qualitatively matched the observed brightening toward the outer boundary of the spiral arm. The relation between β (expressed in units of solar attraction) and v_{eject} (in km/s) was assumed in the form

$$v_{eject} = \frac{\sqrt{\beta}}{A + B\sqrt{\beta}}, \qquad (1)$$

where following some trial-and-error experiment at ion, which was aimed at satisfying the observed expansion of the features, the two constants were chosen to be $A = 7$ s/km and $B = 10$ s/km. The implied peak dust ejection velocity is consistent with the projected expansion velocity of ~ 30 m/s.

The parameters in Table 1 are complemented by Fig. 2, which presents the assumed emission profile of the dust ejecta during each of the three episodes. The emission time, plotted in the figure in relative units, is shown in the table to equal 2 days, so that the production peak is assumed in the model to have occurred about $4\frac{1}{2}$ hours after the event's onset.

The times of dust ejection, derived by fitting the dust emission model to the imaging observations, de.serve further comments. First of all, there is a remarkable correlation among the three emission events: the temporal separation between the first two is 36 days, *exactly* twice the 18 day separation between the last two. It is likely that the 18 day period is closely related to 'the two dynamical constants of the rotation state (the precession and the roll), but at present I will not speculate on details, except to say that if the apparent spin period is *approximately* a submultiple of the 18 day period, it should not be longer than 9-10 days.

COMPUTER SIMULATION OF EVOLUTION OF DUST EJECTA FROM THREE EMISSION EVENTS IN COMET HALE-HOI'I' (LATE AUGUST–LATE OCTOBER 1995)

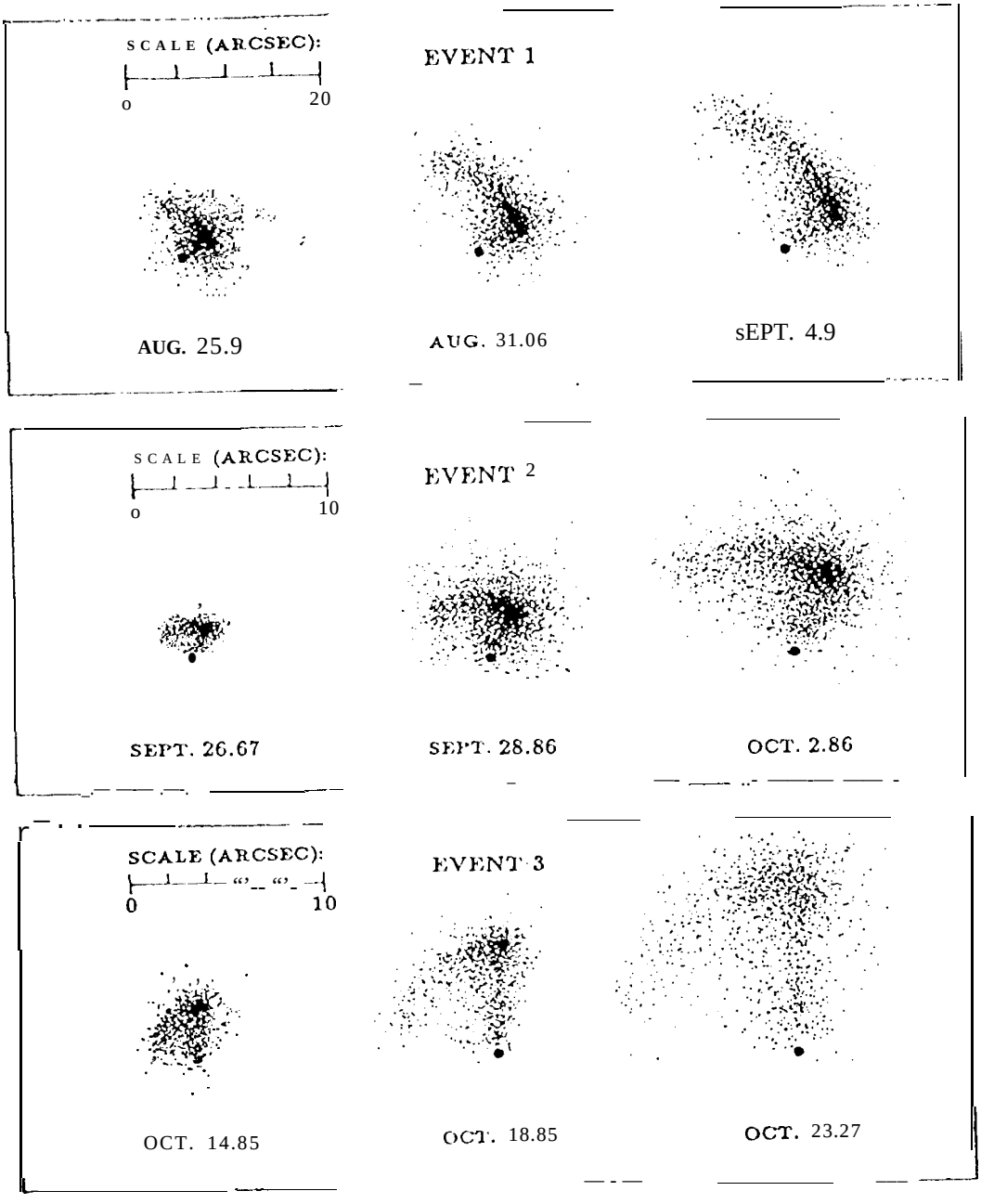

Fig. 1. Synthetic, **computer generated images of comet Hale-Bopp, exhibiting the radial jet and the spiral arm on selected dates following each of the three modelled emission events in late August through** late October. Note that the scale of the images for Event 1 differs from the scales for Events 2 and 3. North is always up and east to the left. The dates are 1995 UT.

Table 1. Computer image simulation of comet Hale Bopp: parameters for emission events in late August through late October 1995.

Parameters common to all emission events			
Dust source:		Dust ejects:	
Apparent cometocentric latitude	0°	Particle acceleration β (units of s.a.)	
Apparent spin period (days)	8	lower limit β_{min}	0.01[a]
Local hour angle of Sun[b]		upper limit β_{max}	0.5
at beginning of emission event	0°	Particle ejection velocity v_{eject} (m/s)	
at end of emission event	+ 90"	lower limit $(v_{eject})_{min}$	12=[c]
Duration of emission event (days)	2	upper limit $(v_{eject})_{max}$	50

Parameters specific to individual emission events	Event 1	Event 2	Event 3
Position of apparent spin axis (equinox J2000.0)			
right ascension of north pole	41°	68"	96"
declination of north pole	-1"	-20°	-2°
obliquity of orbital to apparent equatorial plane	150°	120°	95"
apparent subsolar latitud.	+23°	+30°	+59°
Time of dust ejection from source (1995 UT)			
event onset	Aug. 17.9	Sept. 22.9	Oct. 10,9
event termination	Aug. 19.9	Sept. 24.9	Oct. 12.9

[a] $\beta_{min} = 0.003$ for Event 3.
[b] Reckoned clockwise from meridian of culminating Sun,
[c] $(v_{eject})_{min} = 7$ In/S for Event 3.

The other cornrnent concerns supporting evidence for the onset time of the first event. An activated source on the nucleus surface can fairly easily be recognized even in small instruments by the sudden appearance of a *bright, starlike nucleus condensation*. The so-called ***nuclear magnitudes,*** which describe its prominence, were reported for cornet Hale-Bopp by nine observers between August 5 and 26, a period relevant to Event 1 (Green 1995, O'Meara 1995). Eight of these are visual observers (J. E. Bortle, A. Hale, H. Mikuz, R.J. Medic, C. S. Morris, S. J. O'Meara, P. Roques, and f). A. J. Seargent) and one worked with a CCD detector array (B.E. A. Mueller). For the CCD observation, made through three apertures in the *V* passband, the nuclear magnitude was defined as the magnitude in an aperture of the seeing disk (2 arcsec), to which the observed data were extrapolated. Five of the eight visual observers reported nuclear magnitudes that were almost perfectly consistent, while the estimates by the remaining three were systematically too bright, by 0.3 mag for two of them and by 1 mag for the third one. Pairs of the brightness estimates by two of these observers showed too much scatter, of more than 0.5 mag, and were both averaged. The 21 data points obtained were converted to relative intensities and are plotted in Fig. 3, This "nuclear" light curve shows a major abrupt increase on August 17–18, perfectly coinciding with the event's beginning time inferred in this study from the dust feature's expansion on the images taken between August 25 and September 4. Similar tests will be possible for Events 2 and 3, when the relevant brightness data are available in the other two critical periods. Potentially, similar tests could also be based on photographic data, if they become available.

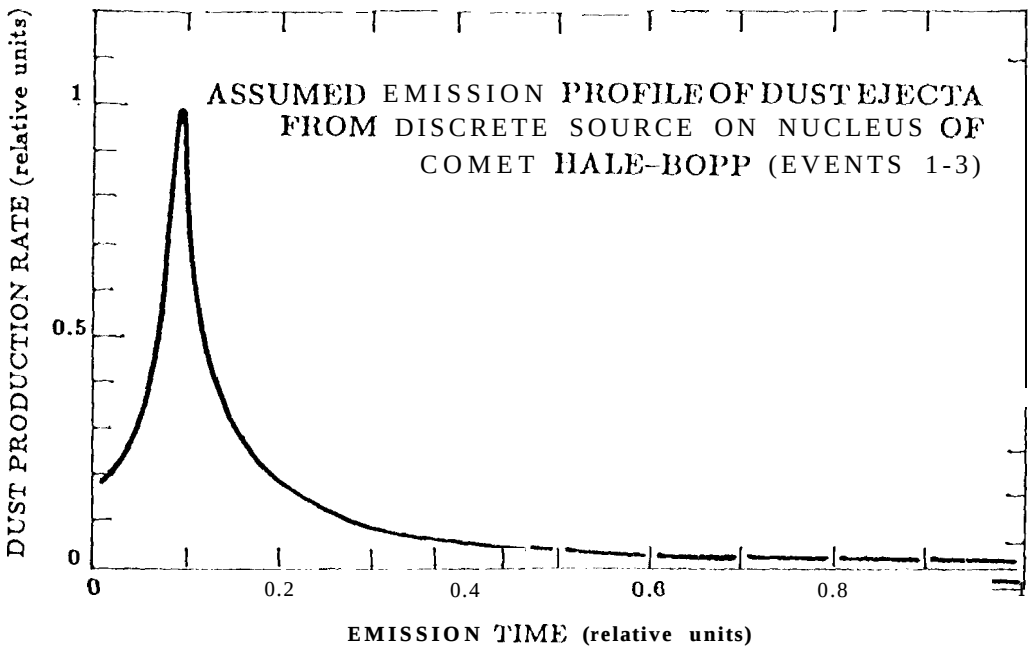

Fig. 2. Emission profile of dust ejects from the discrete source on the nucleus of cornet Hale–Bopp, assumed **in the computer-generated simulations of the dust features that were products of Events 1**, 2, and **3. The time is reckoned from the event's onset. The assumed duration of. each event was 2 days; the peak production rate of dust then occurs** $\sim 4\frac{1}{2}$ **hours after the onset.**

5. The problem of a physical mechanism for the emission events

The visual light curve presented in Fig. 3 provides yet another important information, which is especially useful before more accurate photometric data become available for the observed spiral features. Since in the early days after the termination of Event 1 the '(nuclear condensation" detected by visual observers coincided with the spiral feature displayed on high-resolution images, the difference between the reported limiting brightness levels of the nuclear condensation before and after the event is equal to the total brightness of the spiral feature and, for an assumed geometric albedo, it is diagnostic of the total cross-sectional area of tbe dust ejects in the feature. From Fig. 2 the relevant brightness difference is ~58 units of visual magnitude **16, c,r,** equivalently, magnitude 11 .6. With an assumed geometric albedo of 4 percent, this result implies a projected cross-sectional area of 1.5 x 10^6km2 Consider now a differential distribution law of particle sizes a that varies as $a^{-s}\,da$ between the limiting sizes, $a_{min} \leq a \leq a_{max}$. From the brightness increase in the observed dust features toward their outer boundaries, it was already concluded in Sect. 4 that the power index $s > 5$. In order to assess the uncertainties involved, consider particle size distribution laws for which $4 < s \leq 5\frac{1}{2}$. The ratio between the mass $\mathcal{M}_{dust}$ of dust particles and their cr~s-sections] area $\mathcal{A}_{dust}$ is

$$\frac{\mathcal{M}_{dust}}{\mathcal{A}_{dust}} = \frac{4(s-3)}{3(s-4)} \rho a_{min} \frac{1-(a_{min}/a_{max})^{s-4}}{1-(a_{min}/a_{max})^{s-3}} \qquad (2)$$

for $s > 4$ and

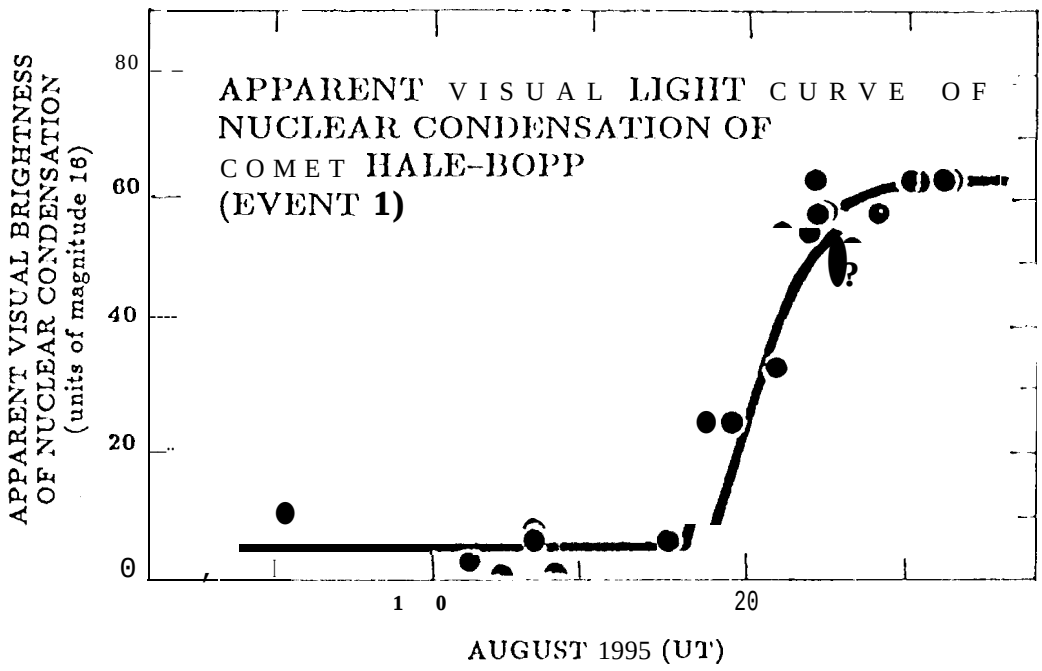

Fig. 3. **Visual light curve of the nuclear condensation of cornet** Hale-Bopp about the time of Event 1. Twenty of the 21 data **points are visual magnitude estimates, one is a** CCD **observation.** 'l'he brightness scale's unit corresponds to an apparent visual magnitude 16.

$$\frac{\mathcal{M}_{\rm dust}}{\mathcal{A}_{\rm dust}} = \frac{4}{3}\,\rho\,\frac{\ln(a_{\rm max}/a_{\rm min})}{1-a_{\rm min}/a_{\rm max}} \qquad (3)$$

for s = 4, where ρ is the dust bulk density, assumed to be independent of particle size. With $\mathcal{A}_{\rm dust} = 1.5 \times 10^{16}$ cm^2, $a_{\rm min} << a_{\rm max}$ and, for example, $\rho a_{\rm min} \simeq 0.1$ g cm^{-3} μm, one has $\mathcal{M}_{\rm dust} \simeq 3.3 \times 10^{11}$ g for s = 5.5 as a probable total mass ejected during Event 1 and $\mathcal{M}_{\rm dust} \simeq 8.7 \times 10^{11}$ g for s = 4.3 as its upper limit (for the given value of the product $\rho a_{\rm min}$). A similar upper limit, $\mathcal{M}_{\rm dust} \simeq 9.2 \times 10^{11}$ g, is provided by taking s= 4 and $a_{\rm max}/a_{\rm min} \simeq 100$. For the Event 1's assumed duration of 2 days, its average dust production rate comes out to be $\mathcal{M}_{\rm dust} \simeq 1.9 \times 10^6$ g/s for the chosen value of $\rho a_{\rm min}$.

Two mechanisms generally considered plausible for explaining sudden episodes of cometary activity at large heliocentric distances are (i) the exothermic transition of water ice from amorphous to cubic phase and (ii) the sublimation of ices, such as carbon monoxide, that are much more volatile than water ice. The first mechanism was proposed by Patashnick et al. (1974) as the energy source for the flare-ups of 29 P/Schwassmann-Wachmann 1; the second mechanism was considered as early as some 40 years ago (Whitney 1955) and carbon monoxide was specifically suggested to be the most likely prime driver that accelerated microscopic dust during a recent major outburst of comet Halley at 14 AU from the Sun (Sekanina et al. 1992). Observational evidence for cornet Hale-Bopp allows one to investigate only the latter option. The 1.3-mm rotational line of carbon monoxide was detected independently by Matthews et al. (1995) *on* September 5, 7, and 19-20 and by Rauer et al. (1995) on August 16 and 23 and September 20--21 (see also Biver et al. 1995). 'l'he line was blueshifted to imply a sunward expansion velocity

of 0.33-0.35 km/s for CO. The two groups reported comparable average CO production rates, $M_{c0} \simeq 7$ to 9 x 10^5 g/s. Sekanina (1995c) noticed that the lower rate is equivalent to a sublimation area of ~ 5 km^2, if near the subsolar point. Although most dates on which CO was detected are outside the critical period for Event 1 and therefore not *directly* comparable with the (highly uncertain) dust production rate estimated above, a very crude assumption of a nearly invariable production of CO leads to a mass loading of the CO flow by dust, that is, to a dust-to-CO production rate ratio of between 1 and 10 in the considered case of $\rho a_{\min} \simeq 0.1$ g cm '3pm, but to a higher mass loading, if the submicron-sized grains do not dominate.

An independent approach to estimating a dust-to-CO production rate ratio is based on Probstein's (1969) model of the interaction of dust and gas in the near-nucleus cometary environment. The (terminal) ejection velocity of a dust particle of radius a and bulk density ρ is in Probstein's theory determined by a dimensionless accommodate ion coefficient α, which is given by

$$\alpha = \frac{8\rho a}{3R\Gamma}\sqrt{c_p T}, \tag{4}$$

where R is the radius of the comet's nucleus and Γ, C_p, and T are, respectively, the mass production rate per unit sublimating area, the specific heat at constant pressure, and the temperature of the gas. I will use for comet Hale-Bopp R = 20 km (Weaver 1995) and, for carbon monoxide, $T = 37$ K and $\Gamma = 1.2 \times 10\text{-s}$ g/cm^2/s, calculated for a heliocentric distance of 6.8 AU from the Antoine constants published by Das et al. (1994), and, as before, $c_p = 1.04$ J/g/deg (Sekanina et al. 1992). Then $\sqrt{c_p T} = 0.196$ km/s and the expression for the accommodation coefficient of dust particles that populate the outer boundary of the spiral feature becomes

$$\alpha_* = 0.22\rho a_{\min}, \tag{5}$$

where ρ is in g/cm^3 and $a_{\min}$ in μm. Since, generally, $\rho \lesssim 1$ g/cm^3 and $a_{\min} \lesssim 1$ μm, one finds that $\alpha_* \ll 1$. In this case, it is possible to make use of Probstein's approximation for the terminal particle-ejection velocity $(v_\psi)_{\lim}$ as a function of the dust mass loading, $\psi = \dot{M}_{\rm dust}/\dot{M}_{\rm CO}$, in the limiting case of $\alpha_* = 0$:

$$(v_\psi)_{\lim} = \sqrt{\frac{2T(c_p + \psi c_{\rm dust})}{1+\psi}}, \tag{6}$$

where $c_{\rm dust} \ll c_p$ is the specific heat of the dust. Since the accommodation coefficient is near, but not equal to, zero, the particle velocity $v_{\rm eject}$ should be somewhat lower than $(v_\psi)_{\lim}$ and one can introduce a correction factor< (slightly smaller than unity), so that

$$v_{\rm eject} = (v_\psi)_{\lim}\,\zeta. \tag{7}$$

The factor ζ can approximately be determined from Probstein's results and the mass loading ψ then follows from

$$\psi = \frac{2c_p T - (v_{\rm eject}/\zeta)^2}{(v_{\rm eject}/\zeta)^2 - 2c_{\rm dust}T}. \tag{8}$$

Since ζ varies slightly with ψ, the relation (8) must be solved iteratively. And since $c_{\rm dust}$ depends on the dust particle composition, which is unknown, the calculations are here limited to the minimum mass loading, $\psi_{\min}$, assuming that $c_{\rm dust}/c_p \to 0$.

It is noted that whether the production ratio ψ is calculated from the photometric considerations, via $\mathcal{M}_{dust}$, or from the particle dynamics, by means of the accommodation coefficient α_*, it always depends on the product ρa_{min}. The common range of the two kinds of solutions can therefore conveniently be determined by plotting ψ versus ρa_{min}, as illustrated in Fig. 4. The photometric solutions are shown for three assumed durations of the emission event, τ_{event}, including the nominal value of 2 days listed in Table 1.

lhe mass loading of the CO flow by the particulate material is found from Fig. 4 to be enormous. To explain the low expansion rate of the spiral feature, the production rate of dust has to exceed the production rate of carbon monoxide by not less--and preferably much more--- than a factor of $\sim$15, as discussed in greater detail in Sect. 6. For an assumed bulk density of 1 g/cm3 the implied minimum (and optically dominant) diameter of the particulate-s in the dust feature is about 1 μm, varying inversely as the density. This result is consistent with the conclusions by Hicks **(1995), which** were based on his color observations of the comet in the near infrared spectral region.

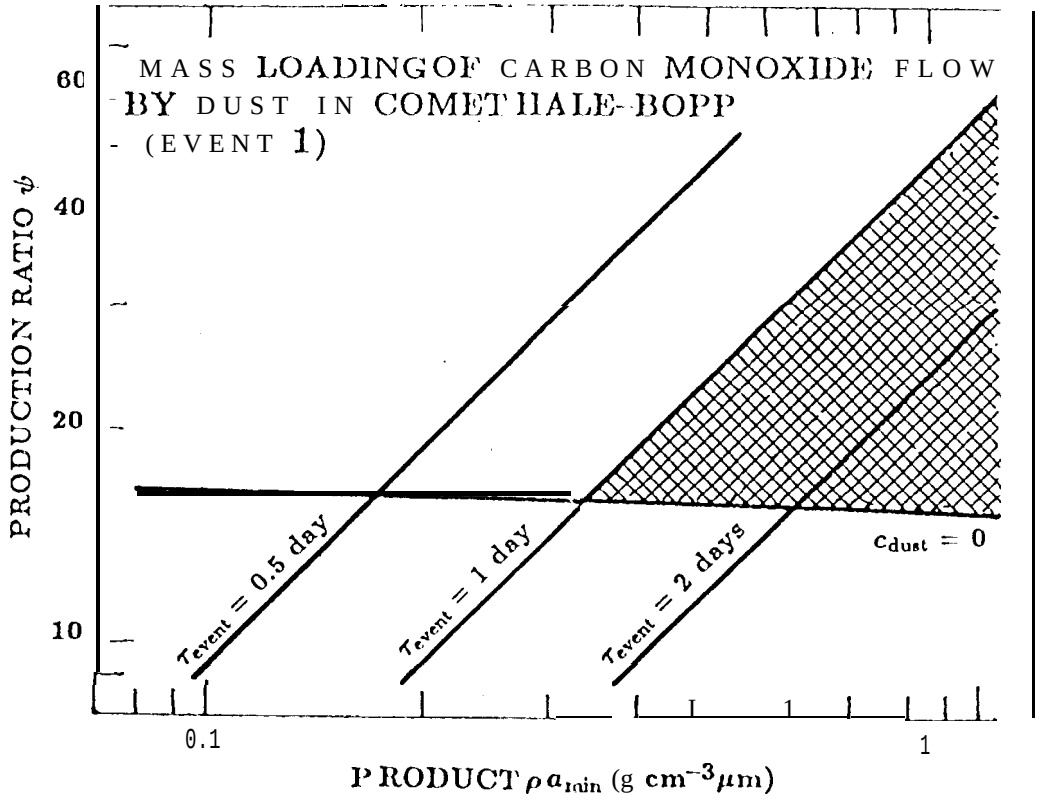

Fig. 4. Mass loading of the flow of carbon monoxide by dust particulate ejected from the nucleus of comet Hale-Bopp during Event 1. The ratio ψ of the mass production rate of dust to the mass production rate of CO is plotted versus the product of of the minimum radius a_{min} of the particles and their bulk density ρ. The nearly horizontal line depicts a crude lower limit to the mass loading ψ, derived from the dust feature's expansion rate on the assumption that c_{dust}, the specific **heat of dust particles, is zero. The photometrically derived solutions for ψ are shown with three assumed durations τ_{event} of Event 1 between** 0.5 and 2 days, although it is unlikely that $\tau_{event} < 1$ day. The **shaded region represents a range of plausible solutions,**

6. Final comments and conclusions

This paper presents an early physical model for comet Hale Bopp. The formulation of a working model at this time, based on information from large heliocentric distances alone, is useful not only for its intrinsic merits but, in the context of long-term modelling efforts, also as a first step that encourages future work.

The cornet's appearance in 1995 was remarkable. At 7 AU from the Sun, the object was unusually bright and its coma was of enormous dimensions, up to 3 million km across. The most prominent feature, observed to recur on three occasions between late August and late October, consisted of a radial, rectilinear jet that made up a sharp boundary of a spiral arm. It is suggested in this paper that the three dust emission events originated from the same discrete source in the equatorial zone of the nucleus and that the feature's characteristic shape was a product of each event's distinct emission profile, with the dust production beginning near local noon, peaking sharply a little later, then gradually subsiding and terminating near local sunset. The temporal separation of 36 days between Events 1 and 2 was exactly twice the interval between Events 2 and 3. This pattern suggests a recurrence period of 18 days and implies that the source failed to activate on at least two occasions, at the end of July and again in early September. Such "ignition duds" are not altogether uncommon in cornets, especially not at large heliocentric distances. In the case of comet Hale Bopp, effects caused by its presumably complex state of rotation (dictated by the systematic variations in the jet's orientation from one event to the next) may also have contributed to the two "skipped" activation cycles. Submultiples of the proposed interval of 18 days are less likely candidates for the recurrence period, because they would imply too many nonevents.

An important category of issues involves the size of the nucleus and the mechanism(s) of the comet's activity at heliocentric distances of more than 6 AU. If Weaver's (1995) preliminary determination of the effective nuclear diameter of ~40 km is confirmed by further observations and analysis, we clearly deal with a larger-than-average cometary object. The CO production rate determinations indicate an outgassing area of ~5–7 km^2, or 0.1-0.15 percent of the estimated total nuclear surface area. For comparison, the production rate of carbon monoxide *from the nucleus* of Halley's comet is known to have amounted to, by number, ≤ 7 percent (Eberhardt et al. 1987, Krankowsky and Eberhardt 1990, Krankowsky 1991) of the production rate of water (Krankowsky et al. 1986), or $\sim 1.8 \times 10^6$ g/s, at the time of the Giotto spacecraft's encounter. With a subsolar CO production rate of 1.54×10^{19} $mol/cm^2/s$, derived from the energy balance equation that involves only sublimation and thermal reradiation effects, Halley's calculated effective outgassing area of CO ice amounted to merely 0.25 km^2, or 0.06 percent of the total nuclear surface area. This compares with a water-ice outgassing area of 36 km^2, or ~10 percent of Halley's surface area (Keller et al. 1987). Thus, in *relative terms*, the effective outgassing area of CO on the nucleus of comet Hale-Bopp near 7 AU from the Sun was about a factor of two *greater* than it had been for Halley at a heliocentric distance of 0.9 AU.

In any case, the comet Hale-Bopp was excessively bright in 1995 not because of its large nuclear size, but because of the apparent existence on its surface of a discrete source that was *both* CO-rich *and* dust-rich and whine areal extent, while very small in comparison with that of the entire nuclear surface, was adequate for the observed effect. One can of course argue that the larger are the dimensions of the nucleus, the higher is the probability for such a source to be activated. Nevertheless, the statistics of recent comets show that CO-rich objects are typically dust poor and *vice* versa.

There is little doubt that the three major events were not Hale–Bopp's only dust-emission episodes. Evidence from various observations (such as changes in the near-nucleus environment on high-resolution images and nearly continuous variations in the brightness of the nuclear condensation) suggests that there ***were*** additional sources of sporadic activity on the nucleus during 1995. More comprehensive analysis of this object's emission pattern will be possible as the database is augmented in due time.

The enormous mass loading of the CO flow try dust calculated for Hale-Bopp is reminiscent of the conclusion reached for the outburst of Halley's cornet at 14 AU from the Sun (Sekanina et al. 1992). Even though seemingly implausible, a dust-mass loading of $\psi \gg 15$ is quite reasonable if one considers that (i) at the relevant heliocentric distances water ice sublimates very insignificantly, thereby behaving essentially as "dust"; (ii) the abundance of CO ice is known to be, at least in Halley-1ike comets, only some 11 percent of the abundance of water ice by mass; and (iii) the total mass of *all* ices may account for less than 50 percent of the ejects's mass (e.g., McDonnell et al. 1991). A dust mass loading equivalent to, say, $\psi \approx 20$ to 30 is not, under these circumstances, excessive. Nevertheless, other mechanisms of dust emission, including the phase change of water ice, should not automatically be dismissed as irrelevant, even though no quantitative tests are available at this time for them in the comet Hale- Bopp's database.

'I'he final set of issues concerns the similarities and differences between the emission patterns displayed by comet Hale–Bopp and by some other comets that are known to have experienced activity at large heliocentric distances. Even without offering details, one can conclude with a great deal of confidence that the appearance and the physical behavior of comets arriving from the Oort cloud (the so called "new" comets) are invariably quite different from the properties of Hale–Bopp. An excellent example of a "new" comet was Howell (1980 E1 = 1982 1) and, before it, some of the objects described by Roemer **(1962), 'I'he heads of these objects are completely or almost completely structureless and their tails are as narrow as, but (usually) significantly longer than, the corns diameter, very much unlike the head and tail of 199501.**

I already compared comet Hale -Bopp with Halley's comet at several places in this study. It appears that the only common points in regard to Halley's outburst at 14 AU from the Sun are an extremely high mass loading of the gas flow by dust and the possibility that carbon monoxide was the driver. The differences are at least three: the diurnal emission profiles are quite different [cf. Fig. 2 in this paper with Sekanina et al.'s (1992) Fig. 5], Halley's outburst was entirely isolated, and, of course, it occurred *after* perihelion and much farther from the Sun.

'The object with which comet Hale–Bopp can most meaningfully be compared is unquestionably P/Schwassmann–Wachmann 1. Distinctive dust structures that remarkably resemble the bright feature recurring near the nucleus of comet Hale–Bopp are not uncommon in Schwassmann–Wachmann 1. The development of the ejecta released during at least two such prominent outbursts in the past 40 years was recorded photographically, in August-September 1957 (Werner 1958) and again in February 1981 (Shao 1981, Shao and Schwartz 1981). The images show that a ring-shaped halo, which made up the bulk of the observed structure, had–- like 1995 C)]—one of its boundaries sharply cut off by a radial jet or fan, while the brightness decreased gradually in the directions away from the jet and the halo terminated on the other side of the nucleus. The azimuthal extent of the ring-shaped envelope was in this case ~250°, not -90° like for Hale–Bopp. A model for the 1981 outburst of Schwassmann–Wachmann 1 (Sekanina 1990, 1993) indicated that the dust production continued for 0.7 the rotation period (independent of the assumed spin rate), because the emission region was in the *circumpolar Sun* regime. In the

scenario proposed in the two papers, the dust source was activated in the late afternoon (the Sun's local hour angle of + 70°), with the production slowly accelerating through midnight (when the Sun was calculated to be less than 20° above the local horizon) and peaking in the morning (at the Sun's local hour angle between –100° and –700), and the event terminated shortly before noon (at the Sun's hour angle of –360). 'l'he emission profile (in Fig. 3 of the]993 paper) is noteworthy, as it closely represents a mirror image of the emission profile proposed in Fig. 2 of this paper for the Hale- Bopp events. 'I'his mirror-like relationship is significant, because there is a ***second solution,*** which is symmetrical to the one explored in the two papers, which requires the opposite sense of nucleus rotation, and which offers an equally good fit to the feature's observed outlines and their expansion with time. In this alternative solution, not considered before, the source is activated in the early afternoon (at the Sun's local hour angle of +36°, the dust production peaks in the late afternoon (at the Sun's hour angle between +70° and +100°), then gradually subsides through midnight, and the event terminates in the early morning (at the Sun's hour angle of –70°). There is now a great deal of resemblance between the emission episodes of the two objects, a conclusion of potentially enormous significance in our quest to understand activity of comets in general and their outbursts in particular. Yet, the emission events in the two comets still differ in some respects, namely, in the rate of occurrence and in the degree of uniformity and temporal evenness. In Schwassmann–Wachmann 1, the flare-up episodes take place rather infrequently and on an entirely irregular basis. In Hale Bopp, they have so far–before the end of 1995–recurred much more often and in a quasi-periodic pattern, whose confirmation or refutal by future observations will be impatiently awaited.

Acknowledgements, 'l'his research was carried out by the Jet Propulsion Laboratory, California Institute of l'ethnology, under contract with the National Aeronautics and Space Administration.

References

Biver, N., Bockelée–Morvan, D., Colom, P., Crovisier, J., Despois, D., Jorda, L., Moreno, R.., Paubert, G., and Rauer, H. 1995, Computer bulletin board report (URL http: //newproducts.jpl.nasa.gov/comet/news7.html)

Das, A., Frenkel, M., Gadalla, N. M., Marsh, K. N., and Wilhoit, R. C., eds. 1994, *TRC **Thermodynamic Tables (Non-hydrocarbons).*** Texas A&M University, College Station, Texas, vol. 5, p. k--1000

Eberhardt, P., Krankowsky, D., Schulte, W., Dolder, U., Lämmerzahl, P., Berthejier, J. J., Woweries, J., Stubbemann, U., Hodges, R. R., Hoffman, J. H., and Illiano, J. M. 1987, A&A 187, 481

Fitzsimmons, A., and Cartwright, M. 1995, IAU Circ. No. 6220

Fomenkova, M, and Mumma, M. J. 1995, IAU Circ. No. 6229 and 6273 (corrigendum)

Green, D. W. E., ed. 1995, ICQ 17, 184

Hicks, M. 1995, IAU Circ. No. 6200

Jewitt, D., and Chen, J. 1995, IAU Circ. No. 6216

Keller, H. U., Delamere, W. A., Huebner, W. II'., Reitsema, H. J., Schmidt, H. U., Whipple, F. L., Wilhelm, K., Curdt, W., Kramm, R., Thomas, N., Arpigny, C., Barbieri, C., Bonnet, R.. M., Cazes, S., Coradini, M., Cosmovici, C. B., Hughes, D. W., Jamar, C., Malaise, D., Schmidt, K., Schmidt, W. K. H., and Seige, P. 1987, A&A 187, 807

Kidger, M. 1995a, IAU Circ. No. 6240

Kidger, M. 1995b, IAU Circ. No. 6244

Kidger, M. 1995c, Astronomer 32, 155

Kidger, M., Serra, M., and Casas, R. 1995, IAU Circ. No. 6220

Krankowsky, D. 1991, in *Comets* in *the Post-Halley Era*, R. L. Newburn, Jr., M. Neugebauer & J. Rahe, eds. (Kluwer, Dordrecht), p. 227

Krankowsky, D., and Eberhardt, P. 1990, in *Comet Halley: Investigations, Results, Interpretations*, J. W. Mason, ed. (Ellis Horwood, Chichester), vol. I, p. 273

Krankowsky, I)., Lämmerzahl, P., Herrwerth, 1., Woweries, J., Eberhardt, P., Dolder, U., Herrmann, U., Schulte, W., Berthelier, J. J., Illiano, J. M., Hodges, R. R., and Hoffman, J. 11.1986, Nature 321, 326

Lidman, C., and Bouchet, P. 1995, IAU Circ. No. 6203

Matthews, H. E., Jewitt, D., and Senay, M. C. 1995, IAU Circ. No. 6234

McDonnell, J. A. M., Lamy, P. J.., and Pankiewicz, G.S. 1991, in Comets *in the Post-Halley Era, R. L.* Newburn, Jr., M. Neugebauer & J. Rahe, eds. (Kluwer, Dordrecht), p. 1043

McNaught, R. H. 1995, IAU Circ. No. 6240

Offutt, W. 1995, IAU Circ. No. 6194

O'Meara, S. J. 1995, ICQ 17, 181

Patashnick, H., Rupprecht, G., and Schuerman, D. W. 1974, Nature 250, 313

Probstein, R. F. 1969, in *Problems of Hydrodynamics and Continuum* Mechanics, F. Bisshopp et al., eds. (Sec. Industr. Appl. Math., Philadelphia), p. 568

Rauer, 11., Despois, D., Moreno, R., Paubert, G., Biver, N., Bockelée-Morvan, D., Colom, P., Crovisier, J., and Jorda, L. 1995, IAU Circ. No. 6236

Roemer, E. 1958, PASP 70, 272

Roemer, E. 1962, PASP 74)351

Sekanina, Z. 1990, AJ 100, 1293, 1389

Sekanina, Z. 1991, in *Comets* in *the Post-Halley Era,* R. L. Newburn, Jr., M. Neugebauer & J, Rahe, eds. (Kluwer, Dordrecht), p. 769

Sekanina, Z. 1993, in *Activity of Distant Comets,* W. F. Huebner, H. U. Keller, D. Jewitt, J. Klinger & R. West, eds. (Southwest Research Institute, San Antonio, TX), p. 166

Sekanina, Z. 1995a, IAU Circ. No. 6194

Sekanina, Z. 1995b, lAU Circ. Nos. 6223, 6240, and 6248

Sekanina, Z. 1995c, IAU Circ. No. 6234

Sekanina, Z. 1996, in *Physics, Chemistry, and Dynamics of the Interplanetary Dust* (ASP Conference Series), in press

Sekanina, Z., Larson, S. M., Hainaut, O., Smette, A., and West, R. M. 1992, A&A 263, 367

Shao, C.-Y. 1981, ICQ 3, 76

Shao, C.-Y., and Schwartz, G. 1981, Sky Telesc. 61, 390

Weaver, H. A. 1995, Computer bulletin board report (URL http://www.arcorp.com/Hale-Bopp.html)

West, R. M. 1995, IAU Circ. No. 6220

Whitney, C. 1955, ApJ 122, 190